



Oh, it was wild and weird and wan, and ever  
in camp o' nights  
We would watch and watch the silver dance of  
the mystic Northern Lights.  
And soft they danced from the Polar sky and  
swept in primrose haze;  
And swift they pranced with their silver feet,  
and pierced with a blinding blaze.

*So wrote Canadian poet Robert W. Service in the "Ballad of the Northern Lights." The northern lights, also known as the aurora borealis, are a product of the complex relationship between the Sun and the Earth.*

*More frequent auroras at more southerly latitudes are evidence of the period of maximum solar activity now upon us. The solar maximum, which occurs approximately every 11 years, also brings with it more active ionospheric conditions. The more frequent ejections of high-energy electromagnetic radiation and particles from the Sun around the time of the solar maximum results in greater ionospheric electron densities and more variable densities. And as the signals from the GPS satellites must pass through this more active ionosphere on their way to Earth-bound receivers, there are potential problems for GPS users. In this month's column, we will look at how solar activity affects the ionosphere, how the ionosphere affects GPS, and how these effects can be ameliorated to reduce their impact.*



# GPS, the Ionosphere, and the Solar Maximum

**Richard B. Langley** University of New Brunswick

The solar maximum is upon us. It brings with it higher and more variable ionospheric electron densities that can try the souls of some GPS receivers. For any ranging system such as GPS, the propagation speed of the signals is of critical importance. This speed, when multiplied by the observed propagation time interval, provides a measure of the range. In the case where an electromagnetic signal propagates in a vacuum, the speed of propagation is the vacuum speed of light — valid for all frequencies. However, the signals transmitted by the GPS satellites must pass through the Earth's atmosphere on their way to receivers on or near the Earth's surface. These signals interact with the constituent charged particles and neutral atoms and molecules in the atmosphere, resulting in a changed propagation speed and direction — the signals are refracted.

When describing atmospheric refraction effects on radio waves, such as GPS signals, it is convenient to separate the effects of neutral atoms and molecules primarily contained in the troposphere (the lowest portion of the atmosphere) from the charged particles principally contained in the ionosphere, the part of the upper atmosphere that is significantly affected by solar activity. In recent "Innovation" columns, such as "Enhancing GPS: Tropospheric Delay Prediction at the Master Control Station" in the January 2000 issue of *GPS World*, we have examined the troposphere's influence on the GPS signals. This month, we turn our attention to the ionosphere.

## THE IONOSPHERE

The ionosphere is the region of the Earth's atmosphere where ionizing radiation primarily in the form of solar extreme ultraviolet (EUV) and x-ray emissions causes electrons to exist in sufficient enough quantities to affect the propagation of radio waves. When the photons that make up the radiation impinge on the atoms and molecules in the upper atmosphere, their energy breaks some of the bonds that hold electrons to their parent atoms. The result is a large number of free, negatively charged electrons as well as positively charged atoms and molecules

called ions. Such an ionized gas is known as a plasma.

The ionosphere is not bound by specific, fixed limits, although the altitude at which the ionosphere begins to be detectable is about 50 kilometers and stretches to heights of 1,000 kilometers or more. The upper boundary of the ionosphere is not well defined as the electron distribution thins out into the plasmasphere (or protonosphere, as the dominant positive ions there are protons) and subsequently into the interplanetary plasma.

As altitude decreases, the ionosphere's absorption of EUV light increases as does the density of neutral atoms and molecules. The net result is the formation of a maximum electron density layer. However, because different atoms and molecules absorb EUV light at varying rates, a series of distinct regions or layers of electron density exist, termed D, E, F1, and F2. The F2 layer is usually where the maximum electron density occurs. The structure of the ionosphere is not constant but is continually varying in response to changes in solar radiation and the Earth's magnetic field. This variability impacts the signals from the GPS satellites as they pass through the ionosphere on their way to users' receivers. Before examining how the ionosphere affects GPS, let's see how the Sun affects the ionosphere.

## SOLAR ACTIVITY

In addition to ultraviolet light and x-rays, the Sun continuously emits a wide spectrum of electromagnetic radiation as well as particle radiation primarily in the form of electrons and protons, called the solar wind. The near-constant level of this radiation deviates by only a small amount. But this variability is quite important, as it directly affects the particles in the ionosphere. Heightened solar activity is characterized by an increase in the number of flares, coronal holes, and coronal mass ejections.

A solar flare is a sudden energy release in the solar atmosphere where electromagnetic radiation, and sometimes energetic particles and bulk plasma are emitted. A sudden increase of x-ray emissions, resulting from a

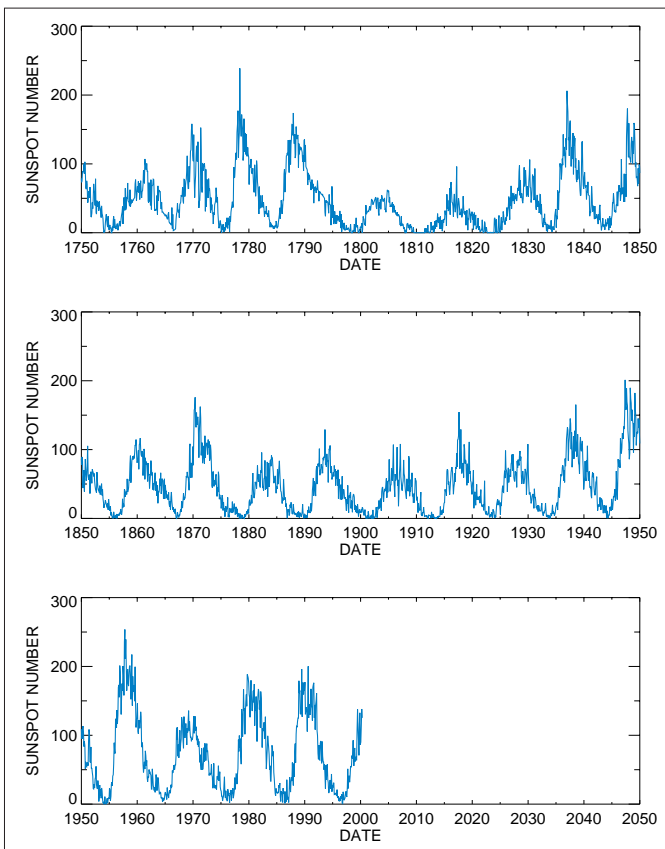


**Figure 1.** Daily observations of sunspots have been carried out since 1749. Initially conducted at the Swiss Federal Observatory in Zürich, the sunspot count is currently computed from observations by an international network of observers. Monthly averages of the International Sunspot Number show that the number of sunspots visible on the Sun waxes and wanes with an approximate 11-year cycle.

flare, causes a large increase in ionization in the lower regions of the ionosphere on the sunlit side of Earth. The x-ray radiation, traveling at the speed of light, takes approximately eight minutes to arrive at the Earth, resulting in an effect soon felt after the flare occurs. High-energy particles can reach the Earth in a fraction of an hour. The lower-energy particles flowing in the solar wind, on the other hand, take two to three days to reach the Earth. Solar flares are usually associated with the strong magnetic fields that manifest themselves in sunspots — relatively cool areas that appear as dark blemishes on the Sun’s face. The sunspots are formed when magnetic field lines just below the Sun’s surface become twisted and poke through the solar photosphere — the visible solar surface.

Sunspots have been observed since at least the early 1600s with regular, daily sunspot counts beginning in 1749. The number of sunspots waxes and wanes with an approximately 11-year periodicity called the solar

23 and near its maximum, shown in Figure 2.

Another sign of increased solar activity are coronal mass ejections (CMEs), huge bubbles of gas threaded with magnetic field lines that are ejected from the Sun. (The corona is the outermost layer of the solar atmosphere). Coronal mass ejections are often associated with solar flares and prominence eruptions. The frequency of CMEs varies with the sunspot cycle. At solar minimum, we observe approximately one CME per week. Near solar maximum, we observe an average of two to three CMEs per day. If a CME is directed toward the Earth, a worldwide disturbance of the Earth’s magnetic field, called a geomagnetic storm, can occur.

**Space weather.** Geomagnetic storms often result in ionospheric disturbances. Magnetic storms and associated ionospheric storms occur when high-energy charged particles from solar flares, prominence eruptions, or coronal holes (regions of exceptionally low-density that show up as dark areas in x-ray

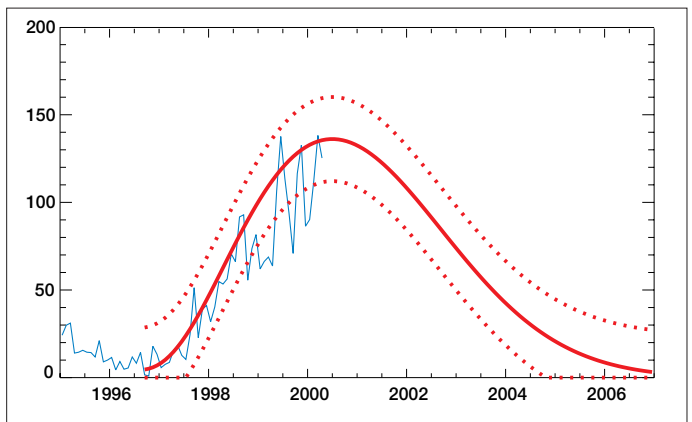


**Figure 2.** The current sunspot cycle, number 23, is predicted to peak this year. Shown in this figure are the observed monthly sunspot averages and the smoothed sunspot count predicted by scientists at NASA’s Marshall Space Flight Center. Also shown by dotted lines is the statistical uncertainty of their predictions.

cycle, shown in Figure 1. Actually, rather than merely counting individual sunspots, solar astronomers compute a sunspot number based on the number of sunspots and sunspot groups. The day-to-day sunspot number can vary widely, so a running average is typically computed to show long-term trends. We are currently in cycle

images of the Sun) arrive at the Earth, causing perturbations in the Earth’s magnetic field. The charged particles interact with the Earth’s neutral atmosphere, producing excited ions and additional electrons. In fact, we can use measurements of the geomagnetic activity as a proxy for ionospheric activity. The strong electric fields that are generated cause significant changes to the morphology of the ionosphere, changing the propagation delay of GPS signals within time intervals as short as one minute. Such changes, primarily in the polar and auroral ionospheres, can last for several hours.

As we noted in the introduction, solar activity is also responsible for the colorful auroras — the northern and southern lights. The Earth is surrounded by a magnetic cocoon (the magnetosphere) created by the interaction of the Earth’s magnetic field with that of the Sun. When the solar wind is particularly strong, it appears to create tears in the cocoon, allowing charged particles trapped in the magnetosphere to enter the ionosphere and spiral down along the Earth’s magnetic field lines. The particles, primarily electrons, interact with oxygen atoms or nitrogen molecules in the atmosphere. Energy from an atom or molecule excited by fast electrons is released as red (oxygen or nitrogen) or green (just oxygen) light.

Figures 3 through 6 illustrate a recent CME and its effect on the Earth’s magnetic field and atmosphere. The CME spawned G4-level magnetic storms (storms or fluctuations in the magnetic field are rated on a scale from 1, or minor, to 5, or extreme) as well as frequent auroras.

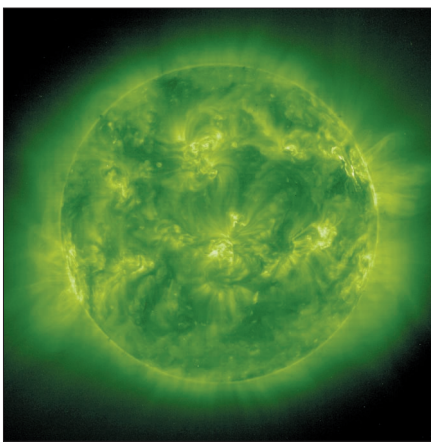


**Figure 3.** On April 4, 2000, at 1541 Coordinated Universal Time (UTC), a magnetically complex sunspot region near the west limb of the Sun produced a large flare that was accompanied by a coronal mass ejection. This image, taken by the Extreme ultraviolet Imaging Telescope (EIT) on the Solar and Heliospheric Observatory (SOHO) spacecraft, shows the active region near the right-side limb at about the two-o'clock position.

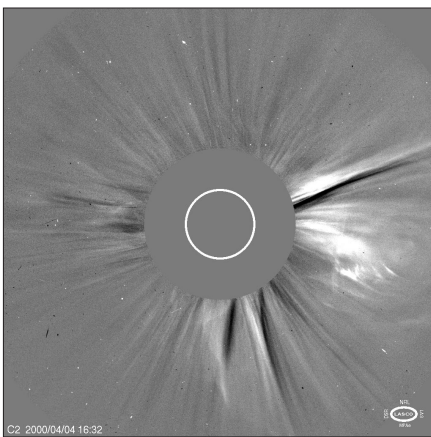


**Figure 4.** The halo coronal mass ejection (CME) which occurred on April 4, 2000 was captured by the Large Angle and Spectrometric Coronagraph Experiment (LASCO) C2 coronagraph on the SOHO spacecraft. This running-difference image, the difference between two sequential images, shows the CME when its leading edge had already left the C2's field of view. The solid-colored disk in the middle is an occulting disk that blocks out the Sun's intense light to reveal the faint corona. The white circle shows the size and position of the Sun.

**REFRACTIVE INDEX**

So how does the ionosphere's behavior, governed by solar activity, affect GPS? To measure the range between a GPS receiver and a satellite, we need to know precisely how fast the radio signals from a satellite propagate. We can characterize the propagation speed of a radio wave (a pure carrier) in a medium such as the ionosphere by its refractive index,  $n$ , which equals the ratio of the speed of propagation in a vacuum (the vacuum speed of light),  $c$ , to the speed in the medium,  $v$ :

$$n = \frac{c}{v} \tag{1}$$

The speed of propagation of a pure or unmodulated wave is actually the speed at which a particular phase of the wave propagates, or the phase speed, and we refer to the refractive index governing this speed as the phase refractive index. A medium may be dispersive, in which case the phase speed is a function of the wave's frequency.

A signal, or modulated carrier wave, can be interpreted as the superposition of a group of waves of different frequencies centered on the carrier frequency. If the medium is dispersive, each of the waves making up the

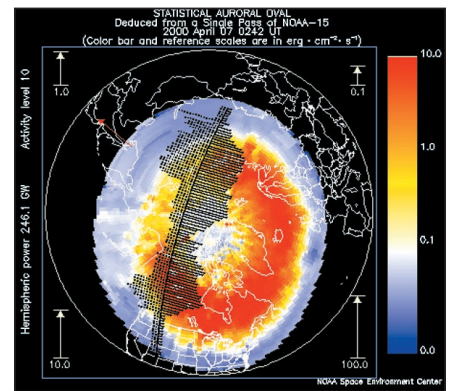


**Figure 6.** When the shock front from the April 4 CME reached the Earth, it triggered auroras that were seen in central Europe and as far south as Florida in North America. This image shows an estimate of the auroral oval on April 7, 2000 at 0242 UTC computed from observations made by the National Oceanic and Atmospheric Administration (NOAA) Polar-orbiting Operational Environmental Satellite (POES), which continually monitors the power flux carried by the precipitating protons and electrons that produce the aurora.

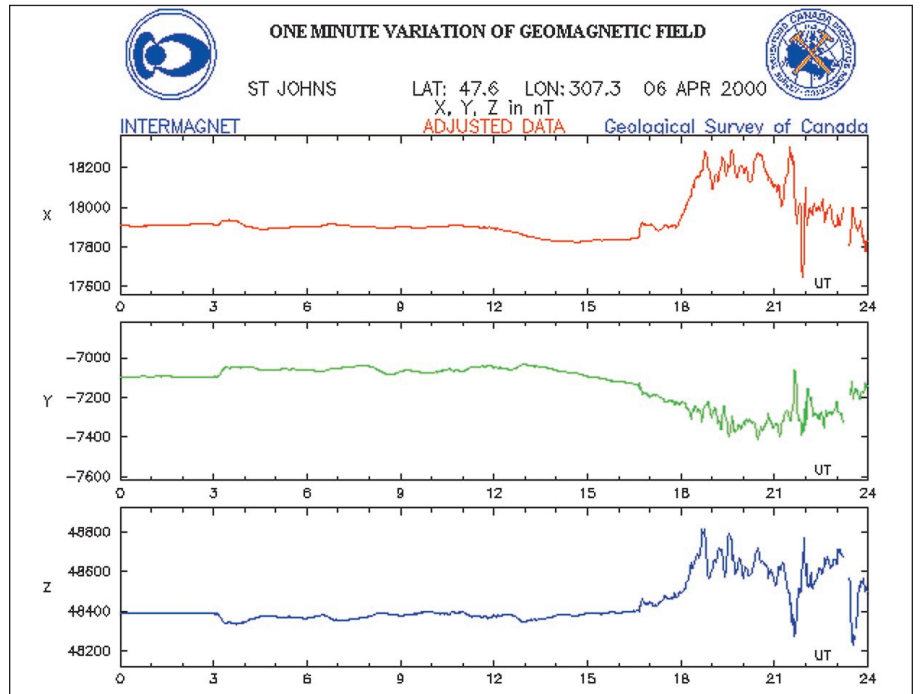


**Figure 5.** The fast-moving material in the CME launched from the Sun on April 4, 2000 arrived at the Earth two days later and generated a geomagnetic storm. Plots of the geomagnetic field components at St. John's, Newfoundland, show a sudden impulse at about 1640 UTC on April 6. The field became quite disturbed shortly thereafter.

group propagates at a different speed. The net result is that the modulation of the signal propagates with a different speed from that of the carrier; this is called the group speed.

Corresponding to the phase refractive index,  $n$ , we can define a group refractive index,  $n_g$ :

$$n_g = \frac{c}{v_g} \tag{2}$$

It can be shown that

$$n_g = n + f \frac{dn}{df} \tag{3}$$

where the derivative,  $dn/df$ , describes how the phase refractive index changes with frequency. In general, a medium will not be homogeneous, in which case,  $n$  and  $n_g$  will be functions of position in the medium.

Because of the varying refractive index, the signal's path through a medium will be bent. The path bending is a direct consequence of Fermat's principle of least time that states out of all possible paths that a radio wave (and other electromagnetic waves such as light) might take, it will take the path that requires the shortest amount of time.

The refractive index of the ionospheric plasma is described by a rather complicated expression developed by Edward Appleton and Douglas Hartree in the early 1930s. The expression assumes an equal number of positive ions and free electrons exist but that the ions (being relatively massive in comparison) have negligible effect on radio waves. In addition to several other constants including the mass and charge of the electron, the refractive index is determined by the electron density, the strength of the Earth's magnetic field, and the frequency of the radio wave. For frequencies significantly higher than the plasma frequency (the "natural" frequency at which ionospheric electrons oscillate, ~ 15–30 MHz), and ignoring the effects of the magnetic field, the expression for the phase refractive index approximates to

$$n = 1 - \frac{40.3 N_e}{f^2} \tag{4}$$

where  $N_e$  is the electronic density in reciprocal cubic meters and  $f$  is the frequency in hertz. Using equation 3, the group refractive index works out to

$$n_g = 1 + \frac{40.3 N_e}{f^2} \tag{5}$$

What are typical values for  $n$  and  $n_g$ ? As we have mentioned, the density of electrons in the ionosphere varies significantly in both space and time. But taking a relatively high value of  $N_e$  of  $10^{12}$  electrons per cubic meter,

$n$  is about 0.9999838 at the GPS L1 frequency, and  $n_g$  is about 1.0000162 — values only slightly different from unity, but nevertheless significant. These refractive index values indicate that the phase speed of a wave in the ionosphere is slightly greater than the vacuum speed of light, while the modulation or group speed is slightly smaller.

The propagation speed of the GPS signals varies all along their path through the ionosphere as the refractive index varies. The signals received by a GPS receiver on or near the Earth's surface are affected by the cumulative or integrated effect of the ionosphere, so the time required for a signal to reach the receiver is given by

$$\tau = \int_S \frac{n'}{c} dS \tag{6}$$

where  $S$  is the path of the signal and  $n'$  is either the phase or group refractive index. We can convert this travel time to an equivalent distance traveled by multiplying it by the vacuum speed of light. Inserting the expressions for the phase and group refractive indices gives us

$$\begin{aligned} \rho_\phi &= c\tau_\phi \\ &= \int_S \left( 1 - \frac{40.3 N_e}{f^2} \right) dS \tag{7} \\ &= \rho - \frac{40.3}{f^2} \int_S N_e dS \end{aligned}$$

and

$$\rho_p = \rho + \frac{40.3}{f^2} \int_S N_e dS \tag{8}$$

where  $\rho$  is the true satellite–receiver geometric range. (We have ignored the small effect the bending of the signal's path has on the measured range.) Carrier-phase measurements of the range are reduced by the presence of the ionosphere (the phase is advanced), whereas pseudorange measurements are increased (the signal is delayed) — by the same amount.  $\int_S N_e dS$  is the integrated electron density along the signal path and is called the total electron content (TEC). TEC is nothing more than a count of the number of electrons in a column stretching through the ionosphere with a cross-sectional area of one square meter.

**TEC VARIABILITY**

TEC is highly variable both temporally and spatially. The dominant variability is diurnal following the variation in incident solar radiation. Maximum ionization occurs at approximately 1400 local time. On the ionosphere's

nighttime side, in the absence of solar radiation, free electrons and ions tend to recombine, thereby reducing the TEC as illustrated in Figure 7. The protonosphere, or uppermost region of the ionosphere, may contribute up to 50 percent of the electron content during the nighttime hours.

Typical nighttime values of vertical TEC for mid-latitude sites are of the order of  $10^{17}$  m<sup>-2</sup> with corresponding daytime values of the order of  $10^{18}$  m<sup>-2</sup>. However, such typical daytime values can be exceeded by a factor of two or more, especially in near-equatorial regions. TEC also varies seasonally with higher values during equinoxes.

Spatially, at latitudes about 20 degrees either side of the geomagnetic equator, high TEC values are produced by a so-called "fountain effect." The effect is caused by drifting electrons interacting with the Earth's magnetic field to produce large-scale movement of ionization. Polar and auroral regions of the ionosphere also have anomalous TEC behavior but for a different reason. Globally, TEC is primarily determined by the Sun's EUV radiation, however some electrons come from the magnetosphere and enter the ionosphere in the auroral regions as mentioned earlier.

Although the Sun emits a broad spectrum of radiation, as we've already discussed, the flux of the Sun's radio emissions at a wavelength of 10.7 centimeters (2.8 GHz) is a useful indicator of solar activity. This particular wavelength was selected for monitoring purposes shortly after World War II, and daily observations have been carried out at observatories in Canada ever since. Recent research has shown that while long-term changes in the 10.7-centimeter solar flux seem to correspond with long-term solar cycle changes in TEC, short-term TEC changes are not well correlated with the day-to-day changes. Only approximately 20 percent of the day-to-day fluctuations in TEC can be attributed to changes in solar EUV. The bulk of TEC changes result from variations in temperature, composition, and dynamics of the ionosphere.

**CORRECTIONS AND MODELS**

So how does a GPS receiver cope with the ionosphere both when it is quiescent or well-behaved and when it is active?

As we noted, both pseudorange and carrier-phase observations are biased by the presence of the ionosphere. This bias must be accounted for or position accuracy will suffer. Dual-frequency receivers take advantage of the ionosphere's dispersive nature to correct for its effect. A linear combination of the

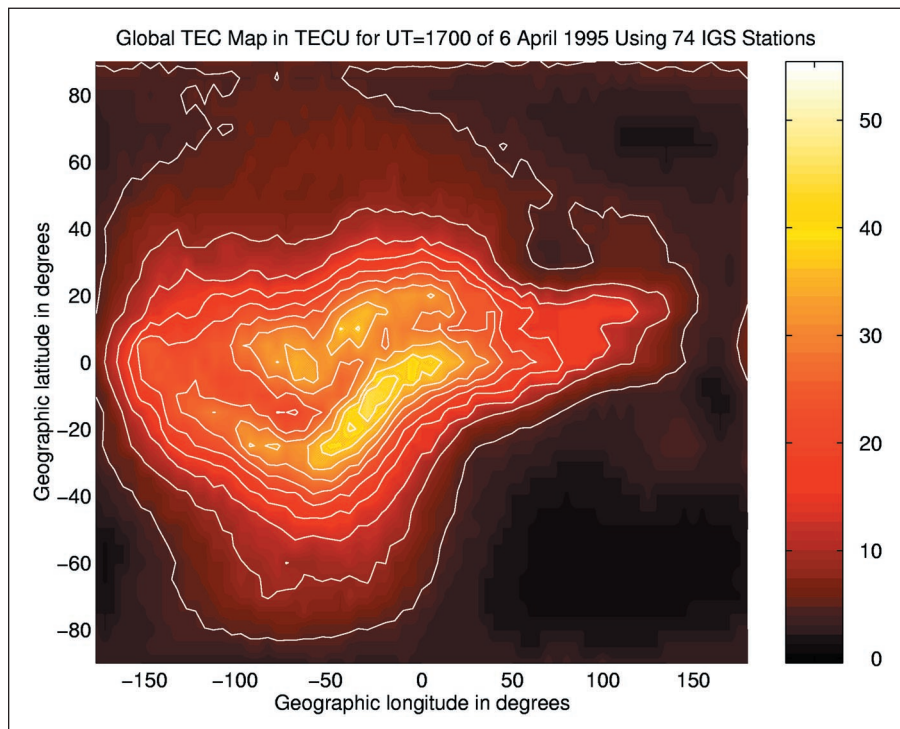


**Figure 7.** A “snapshot” of the global total electron content (TEC) at 1700 UTC on April 6, 1995, clearly shows the ionosphere’s diurnal behavior and the equatorial anomaly spanning either side of the geomagnetic equator. Contours are in total electron content units (1 TECU = 10<sup>16</sup> electrons per square meter). The map was computed using data from 74 stations of the International GPS Service network.

L1 and L2 pseudorange measurements may be formed to estimate and subsequently remove almost all the ionospheric bias from the L1 measurements:

$$d_{ion,1} = \frac{f_2^2}{f_2^2 - f_1^2} [P_1 - P_2] + e \quad (9)$$

where  $f_1$  and  $f_2$  are the L1 and L2 carrier frequencies respectively,  $P_1$  and  $P_2$  are the L1 and L2 pseudorange measurements, and  $e$  represents random measurement errors and other biases such as satellite and receiver inter-frequency biases. (It is also possible to directly compute an ionosphere-free combination without the extra step of first computing the ionospheric delay.) A similar approach is used to correct carrier phase measurements with

$$d_{ion,1} = \frac{f_2^2}{f_2^2 - f_1^2} \left[ (\lambda_1 N_1 - \lambda_2 N_2) - (\Phi_1 - \Phi_2) \right] + e \quad (10)$$

where  $\Phi_1$  and  $\Phi_2$  are the L1 and L2 carrier-phase measurements (in units of length) respectively,  $\lambda_1$  and  $\lambda_2$  are the L1 and L2 carrier wavelengths respectively,  $N_1$  and  $N_2$  are the L1 and L2 integer cycle ambiguities respectively, and  $e$  represents random mea-

surement errors and other biases.

In practice,  $N_1$  and  $N_2$  cannot be determined, but as long as the phase measurements are continuous (no cycle slips) they remain constant. Hence, the carrier-phase measurements can be used to determine the variation in the ionospheric delay — the so-called differential delay — but not the absolute delay at any one epoch. The estimation of the differential delay in this way, having ignored third and higher order effects in the expressions for the refractive indices, is accurate to a few centimeters. For higher accuracy we would need to account for the higher order terms neglected in the first order approximation, including the geomagnetic field effect as well as ray path bending.

If measurements are made at only one carrier frequency, then an alternative procedure for correcting ionospheric bias must be used. The simplest approach, of course, is to ignore the effect. Surveyors sometimes follow this approach by employing relative positioning over short distances using single frequency GPS receivers. Differencing between the observations by simultaneously observing receivers removes that part of the ionospheric range error that is common to the measurements at both stations. The remain-

ing residual ionospheric range error results from the fact that the signals received at the two stations have passed through the ionosphere at slightly different elevation angles. Therefore, the TEC along the two signal paths is slightly different, even if the vertical ionospheric profile is identical at the two stations.

In differential positioning, the main result of this effect is a baseline shortening proportional to the TEC and proportional to the baseline length. Such errors can introduce significant scale and orientation biases in relative coordinates. For example, at a typical mid-latitude site using an elevation cut-off angle of 20 degrees, a horizontal scale bias of -0.63 parts per million is incurred for each  $1 \times 10^{17} \text{m}^{-2}$  of TEC not accounted for. Nevertheless, ignoring the ionospheric effect on very short baselines may be preferable to the use of the dual-frequency linear combination and the attendant higher observation noise.

An empirical model also can be used to correct for ionospheric bias. The GPS broadcast message, for example, includes the parameters of a simple prediction model. While this model can sometimes account for approximately 70 to 90 percent of the daytime ionospheric delay, it was designed to remove only about 50 percent of the delay on a root-mean-square basis. More sophisticated ionospheric models, such as the Bent Ionospheric Model and the International Reference Ionosphere, may not perform much better than the broadcast model in part because the top portion of the ionosphere is inaccurately represented. An estimate of solar activity drives these models. In the case of the broadcast model, a running average of the observed solar flux values for the past five days is used. But as we noted, the day-to-day variability of the ionosphere is not well correlated with variations in the flux.

Ionospheric delay corrections can be computed by a regional network of dual-frequency receivers and transmitted in real-time to single-frequency users by radio transmissions or archived for data postprocessing. This technique is used, for example, by Natural Resources Canada for their GPS•C service and will be used for the Federal Aviation Administration’s Wide Area Augmentation System.

**IONOSPHERIC SCINTILLATION**

If the number of electrons along a signal path from a satellite to a receiver changes rapidly, the resulting rapid change in the phase of the carrier may present difficulties for the carrier tracking loop in a GPS receiver. For a GPS receiver tracking the L1 signal, a change of

only 1 radian of phase (corresponding to  $0.19 \times 10^{16} \text{ m}^{-2}$  change in TEC, or only 0.2 percent of a typical  $10^{18} \text{ m}^{-2}$  TEC) in a time interval equal to the inverse of the receiver bandwidth can be enough to cause problems for the receiver's tracking loop. If the receiver bandwidth is only 1 Hz (which is just wide enough to accommodate the geometric Doppler shift), then when the second derivative of the phase exceeds 1 Hz per second, loss of lock will result. During such occurrences, the signal amplitude also generally fades.

These short-term (less than 15 seconds) variations in the signal's amplitude and phase are known as ionospheric scintillations. Scintillation effects are most pronounced in the early evening hours and may affect GPS receivers differently, depending on their hardware and software differences. Some codeless dual-frequency receivers, for example, are particularly susceptible to loss of lock problems on the L2 signal when rapid fluctuations exist in ionospheric electron content. Generally, receivers making carrier-phase measurements are more susceptible to scintillations than code-only receivers.

A temporary loss of lock results in a phase discontinuity or cycle slip. A cycle slip must be repaired before the data following the slip can be used. Large variations in ionospheric range bias during short time

intervals can hamper the determination of the correct number of integer cycles associated with these phase discontinuities. If the variations of the ionospheric range bias exceed one half of a carrier cycle, they may be wrongly interpreted in the data processing as a cycle slip.

**Signal fading.** Two regions exist where irregularities in the Earth's ionosphere often occur causing short-term signal fading that can severely test the tracking capabilities of a GPS receiver: the region extending approximately  $\pm 20$  degrees either side of the geomagnetic equator and the auroral and polar regions. The fading can be so severe that the signal level drops completely below the receiver's signal lock threshold. When this occurs, data are lost until the receiver reacquires the signal. The process of loss and reacquisition of signals may go on for several hours.

Such signal fading is also associated with geomagnetic storms. Occasionally, magnetic storm effects extend to the mid-latitudes. During the storm that occurred in March 1989, during the previous solar maximum, range-rate changes produced by rapid variations in TEC exceeded 1 Hz in one second. As a result, GPS receivers with a narrow 1 Hz bandwidth continuously lost lock during the worst part of the storm because of their inability to follow the changes.

## FURTHER READING

To learn more about solar activity and the ionosphere, see

- *Handbook of Geophysics and the Space Environment*, edited by A.S. Jursa, the Air Force Geophysics Laboratory, Hanscom AFB, Massachusetts, 1985.

- *Introduction to the Space Environment*, 2nd edition, by T. F. Tascione, Krieger Publishing Company, Malabar, Florida, 1994.

- "Eye on the Ionosphere," a column in *GPS Solutions*, published quarterly by John Wiley & Sons, Inc., New York.

For previous "Innovation" columns about the ionosphere, see

- "Ionospheric Effects on GPS," by J.A. Klobuchar, *GPS World*, Vol. 2, No. 4, April 1991, pp. 48–51.

- "GPS — Satellites of Opportunity for Ionospheric Monitoring," by D. Coco, *GPS World*, Vol. 2, No. 9, October 1991, pp. 47–50.

- "Effects of the Equatorial Ionosphere on GPS" by L. Wanninger, *GPS World*, Vol. 4, No. 7, July 1993, pp. 48–54.

For a comprehensive analysis of how the ionosphere affects GPS and how GPS can be used to study the ionosphere, see

- "GPS and the Ionosphere," by A.J. Mannucci, B.A. Iijima, U.L. Lindqwister, X. Pi, L. Sparks, and B.D. Wilson, Chapter 25 in *Review of Radio Science: 1996-1999*, edited by W.R. Stone for the International Union of Radio Science, Oxford University Press, 1999; pp. 625–665.

There is a wealth of current and interesting material about space weather and the solar maximum on the World Wide Web, for example

- Space Environment Center, National Oceanic and Atmospheric Administration (providing space weather alerts and warnings and related educational material) <<http://www.sec.noaa.gov/>>.

- SpaceWeather.com (science news and information about the Sun-Earth environment) <<http://www.spaceweather.com/>>.

- Sunspots and the Solar Cycle (data and background information on cycle #23) <<http://www.sunspotcycle.com/>>.

- Solar Data Analysis Center at NASA Goddard Space Flight Center (the latest ground- and space-based solar images) <<http://umbra.nascom.nasa.gov/>>.

- International Solar-Terrestrial Physics (exploring the Sun-Earth connection during solar maximum) <<http://www-istp.gsfc.nasa.gov/>>.

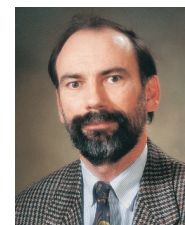
## CONCLUSION

The solar maximum seems to be upon us. In recent months, we have witnessed a significant increase in solar activity with frequent solar outbursts and the attendant effects on the Earth's magnetic field and ionosphere. Although the auroras are the most visible effects of this solar activity, we also witness the impact on the various infrastructures of our modern society: spurious currents in electricity grids and pipelines, increased atmospheric drag on low-orbiting spacecraft, and potential damage to the equipment on communications satellites. The signals from GPS satellites also can be significantly affected. At best, predictive ionospheric models lose their accuracy; at worst, a receiver may not even be able to track the signals.

But a silver lining for GPS does exist. The higher and more variable total electron content values offer scientists an enhanced opportunity to study the ionosphere and its complex relationship with solar activity. And with better understanding of the ionosphere and further improvements in hardware and software, at the next solar maximum in about 11 years' time, GPS receivers may be better able to weather the space storms that it will inevitably bring.

## ACKNOWLEDGMENTS

The figures used to illustrate this article were kindly provided by the Solar Physics Group of Marshall Space Flight Center's Space Science Department (Figures 1 and 2); the SOHO EIT and LASCO consortia (Figures 3 and 4); the Geological Survey of Canada (Figure 5); the Space Environment Center, National Oceanic and Atmospheric Administration (Figure 6); Attila Komjathy, University of Colorado (Figure 7). Thanks to Anthea Coster for helpful comments on a draft of this article. ■



"Innovation" is a regular column featuring discussions about recent advances in GPS technology and its applications as well as the fundamentals of GPS positioning. The

column is coordinated by Richard Langley of the Department of Geodesy and Geomatics Engineering at the University of New Brunswick, who appreciates receiving your comments as well as topic suggestions for future columns. To contact him, see the "Columnists" section on page 4 of this issue.